EEET ECOLOGICAL ENGINEERING & ENVIRONMENTAL TECHNOLOGY

*Ecological Engineering & Environmental Technology*, 2025, 26(5), 43–52
https://doi.org/10.12912/27197050/202691
ISSN 2719–7050, License CC-BY 4.0

Received: 2025.01.31
Accepted: 2025.03.24
Published: 2025.04.01

# Drip irrigation modelling for young cork oaks in Maâmora forest (Morocco)

Abderrafya Mitique[1], Abderrahim Hmimou[2], Yassyr Draoui[1], Mohammed Igouzal[1*]

[1] Laboratory of Electronic Systems, Information Processing, Mechanics and Energy, Ibn Tofail University, 14000 Kenitra, Morocco
[2] Laboratory of Research Team RIPA (Innovative Research and Applied Physics), Department of Physics, Moulay Ismail University, B.P 11201, Zitoune, Meknes, Morocco
* Corresponding author's e-mail: Mohammed.igouzal@uit.ac.ma

## ABSTRACT

The Maâmora forest in Morocco, the world's largest cork oak (Quercus suber) forest, faces significant threats from drought, urbanization (driven by its proximity to major cities like Rabat and Kenitra), tree debarking, and overgrazing. This leads to an increase of tree mortality. Reforestation attempts have been made in several places, but their results have been unsuccessful because young trees could not withstand drought and climate change. To address these challenges, sustainable irrigation methods are crucial for mitigating dieback, promoting seedling growth, and improving tree health. This study evaluated the effectiveness of drip irrigation in enhancing water use efficiency for promoting young cork oaks growth in a specific site of the studied area (475 km$^2$). Soil properties were analyzed using granulometer and disc infiltrometer tests in five sites, revealing a predominantly sandy texture (95–99%), a water flux of 0.56 cm/h and a saturated hydraulic conductivity of 0.0088 cm/s. Spatial interpolation of soil texture was accomplished with GIS and water flow was simulated using the HYDRUS-2D numerical model. The study reveals that the sandy soils of the Maâmora forest exhibit very low initial water content (initial moisture is 0.012 cm$^3$/cm$^3$), highlighting their vulnerability to drought. Numerical simulations demonstrated that drip irrigation effectively distributes water, with moisture reaching depths of up to 240 cm after 400 hours, ensuring adequate hydration for cork oak seedlings. The study underscores the importance of integrating numerical modeling and GIS-based soil mapping to develop sustainable irrigation practices, reducing seedling mortality and enhancing forest resilience under climate change.

**Keywords:** Maâmora forest, unsaturated soil, hydrodynamic parameters, HYDRUS-2D, irrigation.

## INTRODUCTION

The Maâmora forest (northwest of Morocco) is one of the largest woodlands in the Mediterranean (Laaribya et al., 2021). Its significance lies not only in its vast area but also in its vital role in supporting local and regional economic and social activities (Hracherrass et al., 2009). The Maâmora forest extends up to 70 kilometers inland along the Atlantic Ocean between Rabat and Kenitra, with an area of 133,000 hectares, including 64,000 hectares of cork oak (Laaribya et al., 2006; Cherki et al., 2011). It is bordered to the south by the Bouregreg valley and the foothills of the central plateau, and to the north by the Gharb plain (Boukbida et al., 2016). It thrives in acidic soils derived from granite, schist, or sandy substrates (Serrasolses et al., 2009; Poeiras et al., 2021). Cork oak forests and the derived silvopastoral systems play important role in preventing desertification (Aronson et al., 2009; Camilo-Alves et al., 2020). However, in recent years, the Maâmora forest has witnessed a concerning rise in cork oak mortality rates. Cork oak dieback is a complex, multifactorial phenomenon, with drought identified as a primary driver of tree decline (Boukbida et al., 2016; Gliti et al., 2023), and also human pressures as deforestation, overgrazing and urbanization (Benabou et al., 2022). Extensive degradation arrives especially in the areas where natural regeneration is insufficient. To counteract this, targeted reforestation and restoration efforts have been implemented, including the use of supplemental irrigation in localized areas to maintain young cork oak trees. This approach, though unconventional for forests in arid regions where water scarcity is a pressing concern, is necessary to preserve the ecological integrity. The scientific problem of this paper lies in understanding the effectiveness of local irrigation in promoting the growth of young cork oaks, specifically for their use in reforesting vulnerable areas. The authors expected that by using irrigation in targeted zones, they could enhance regeneration, support reforestation efforts, and ultimately improve the ecological resilience of the forest in the face of climate challenges. This study sought to bridge critical knowledge gaps by integrating in situ soil measurements, GIS, and HYDRUS-2D modeling for designing efficient irrigation strategies, in term of cork oak distribution and drip irrigation scenario. This method will help to understand the various interactions and environmental responses, despite their complexity, and assist in making informed decisions regarding the areas to be irrigated, the quantity of water to be used, and the distribution of young cork oak.

## MATERIALS AND METHODS

### Numerical modeling

Soil water movement in the experiment field was simulated as water flow in a 2D vertical plane that crosses a drip emitter. The governing equation for water flow is as follows (Brunetti et al., 2020; Bourziza et al., 2017).

$$\frac{\partial \theta}{\partial t} = \frac{\partial \theta}{\partial h}\frac{\partial h}{\partial t} = \frac{\partial}{\partial x}\left(K(h)\frac{\partial h}{\partial x}\right) + \frac{\partial}{\partial z}\left(K(h)\left(\frac{\partial h}{\partial z} - 1\right)\right) \quad (1)$$

where: $\theta$ is the volumetric water content ($cm^3 \cdot cm^{-3}$), $h$ is the pressure head ($cm$), and $K(h)$ is the unsaturated hydraulic conductivity function ($cm \cdot day^{-1}$). Soil hydraulic properties were estimated with the van Genuchten-Mualem function, which is as follows:

Van-Genuchten expression for $\theta(h)$ (Van Genuchten et al., 2014; Giuseppe et al., 2007):

$$\theta(h) = \theta_r + (\theta_s - \theta_r)[1 + |\alpha h|^n]^{-m} \quad (2)$$

The expression of Brooks and Corey was used for function $K(\theta)$ (Brooks et al., 1994):

$$K(\theta) = K_s\left(\frac{\theta(h) - \theta_r}{\theta_s - \theta_r}\right)^{\eta} \quad (3)$$

where: $\theta_s$($cm^3 \cdot cm^{-3}$) is the saturated water content; $\theta_r$($cm^3 \cdot cm^{-3}$) is the residual soil water content; $h$ is the soil water pressure head; $K_s$ (cm/s) is the saturated hydraulic conductivity; $\eta$(-) is the shape parameter; $\alpha$, $n$ and m are the model parameters, with (m = 1 - 1⁄n) (Qanza et al., 2018).

HYDRUS-2D model has been extensively tested and validated in numerous studies, ensuring its reliability and credibility in scientific research (Šimůnek et al., 2006; Bufon et al., 2012). It excels in modeling two-dimensional movement of water in variably saturated soils, making it highly suitable for the studies involving irrigation, soil-water interaction, and plant growth. This software applies the Richards equation (equation 1) to model unsaturated water flow and transport, using Galerkin finite element method (Jiří Šimůnek et al., 2024; Skaggs et al., 2004). The use of HYDRUS-2D in the conducted study emphasizes its ability to simulate irrigation scenarios for young cork oaks, addressing questions about optimal water usage, distribution patterns, and environmental impacts. On other hand, the limitations of HYDRUS-2D can be related to the complexity of input data, since accurate simulations require detailed input data, including soil hydraulic properties, root distribution, and climatic parameters. Obtaining this data can be time-consuming and challenging in heterogeneous environments. Also, HYDRUS-2D relies on certain assumptions, such as homogeneous soil layers and isotropic conditions, which may not fully represent complex natural systems like forests. Finally, while effective in simulating soil-water dynamics, applying HYDRUS-2D to large-scale irrigation planning may require simplifications, potentially overlooking local variations in soil and vegetation interactions.

### Study site

The Maâmora forest is situated in the North-West of Morocco, spanning up to 70 kilometers inland along the Atlantic Ocean between Rabat and Kenitra (Lemkimel et al., 2024). It is bordered to the south by the Bou Regreg valley and the foothills of the central plateau, and to the north by the

Gharb plain (Ghouldan et al., 2024). Covering an area of 133,000 hectares, including 64,000 hectares of cork oak (Cherki et al., 2011; Laaribya et 2021). It serves various social, economic, environmental, and recreational purposes. For this study, the West Maâmora forest region was selected as the primary research area, encompassing an area of 475 square kilometers. Figure 1 illustrates the study area of the West Maâmora forest.

## Measurement of soil physical properties

Soil samples of 250 cm³ were collected in five sites under investigation (Saknia, Taicha, Sidi Allal El Bahraoui, Lahemassisss and Aarjate) in order to calculate dry bulk density $\rho_d$, initial mass water content $\theta_{i,m}$ and initial volumetric water content $\theta_i$ (Table 1). The very low value of initial moisture content indicates that soils are initially extremely dry, and these values, along with the apparent density values, suggest that the studied soil is sandy.

Then, a disc infiltrometer with a 20 cm diameter and a reservoir of 6 cm diameter was used to measure hydrodynamic properties of unsaturated soil near saturation (Fig. 2) (Fatehnia et al., 2014; Mitique et al., 2024). For each of the five sites under investigation 9 to 10 tests, were conducted, with experiment lasting between 2 and 30 minutes. Each test involved setting a pressure value ($h_0$) between -20 cm and 0 cm, and recording drop in water level in the reservoir is during infiltration. This allows calculating cumulative infiltration ($I$), water content $\theta$ and hydraulic conductivity $K$. Once the experiment is completed, soil samples are taken from the soil layer beneath the disc to determine the water content associated with the applied pressure. These samples are placed in airtight bags, brought to the laboratory, weighed, dried in an oven at 105 °C for 48 hours to evaporate all water, and weighed again. Hydrodynamic parameters ($\theta_r$, $\theta_s$, $n$, $a$, $K_s$, $\eta$) can be determined by fitting the Van-Genuchten $\theta(h)$ and Brooks & Corey $K(\theta)$ models (Equation 2 and 3) to the experimental points of the five soils in the study area (Table 2).

The granulometric method was used to determine the texture of the soil under study, providing crucial information about its composition. This method is based on sieving with a series of stacked

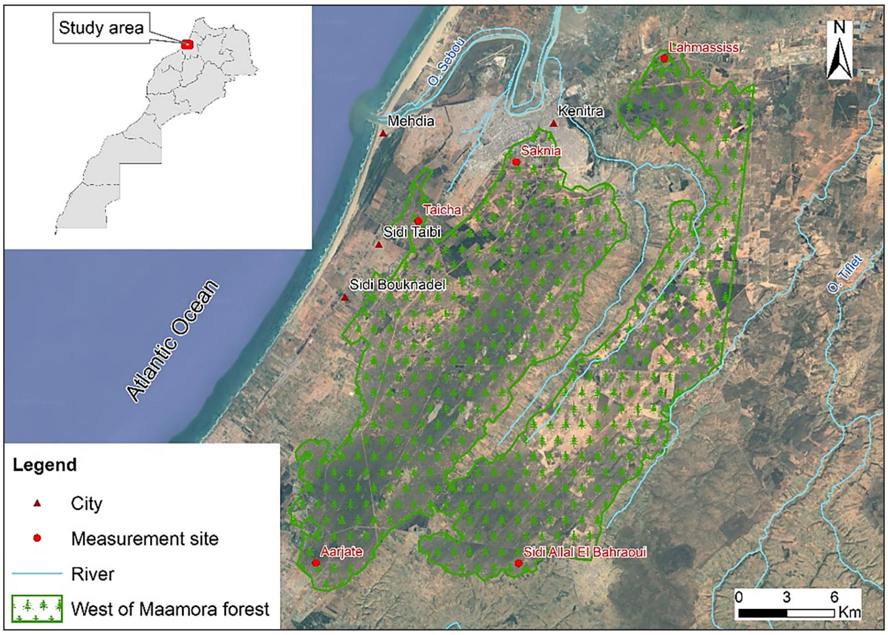


**Figure 1.** Geographical situation of the western part of the Maâmora forest

**Table 1.** Dry bulk density and initial water content values of the five soils studied.

| Parameters | Values | | | | |
|---|---|---|---|---|---|
| | Saknia | Taicha | Sidi Allal El Bahraoui | Lahemassisss | Aarjate |
| $\theta_d$(g·m$^{-3}$) | 1.5648 | 1.698 | 1.5228 | 1.55 | 1.508 |
| $\theta_i$(cm$^3$· cm$^{-3}$) | 0.01199 | 0.01159 | 0.0144 | 0.0044 | 0.0072 |

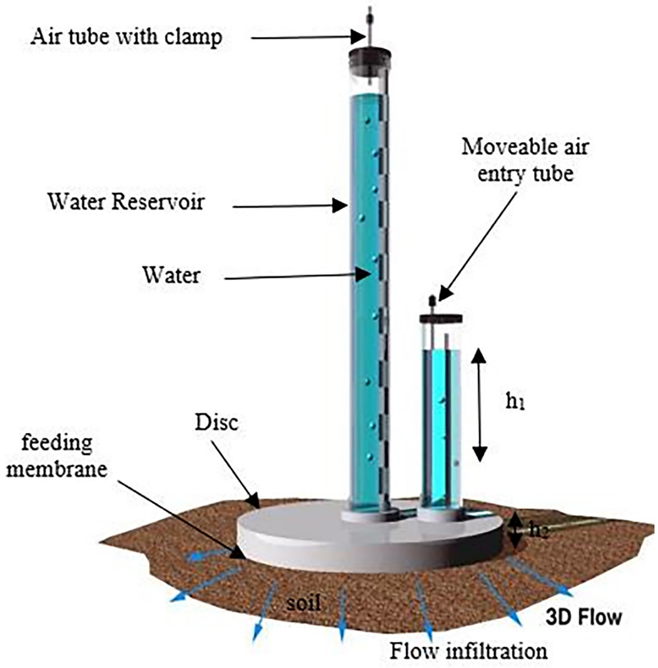


**Figure 2.** The disc infiltrometer

**Table 2.** Adjusted hydrodynamic parameters of the five soils studied

| Hydrodynamic parameters | Saknia | | Taicha | | Sidi Allal El Bahraoui | | Lahemassiss | | Aarjate | |
|---|---|---|---|---|---|---|---|---|---|---|
| | Value | $R^2$ | Value | $R^2$ | Value | $R^2$ | Value | $R^2$ | Value | $R^2$ |
| $\theta_r$(cm³· cm⁻³) | 0 | 0.95 | 0 | 0.94 | 0 | 0.85 | 0 | 0.95 | 0 | 0.91 |
| $\theta_s$(cm³· cm⁻³) | 0.31151 | | 0.32453 | | 0.38785 | | 0.30342 | | 0.358 | |
| $n$(-) | 2.73577 | | 2.15389 | | 2.00306 | | 2.75827 | | 1.57747 | |
| $\alpha$(cm⁻¹) | 0.05367 | | 0.09906 | | 0.09298 | | 0.0792 | | 0.15402 | |
| $K_s$ (cm/s) | 0.0088 | 0.83 | 0.0053 | 0.82 | 0.00209 | 0.91 | 0.01101 | 0.83 | 0.0145 | 0.89 |
| $\eta$ | 3.313 | | 5.18027 | | 1.64983 | | 6.20576 | | 3.21849 | |

sieves with different mesh size. This arrangement allows the particles to be sorted according to their diameter, thus providing a detailed analysis of the particle size distribution of the soil (Ballais et al., 2007; Vdović et al., 2010). On a different note, the spatial interpolation method and GIS were employed to map and evaluate the spatial distribution of soil texture in the Maâmora Forest at different depths: 0-20 cm, 20-40 cm, 40-60 cm, and 60-80 cm, particularly in the western part of the forest. The use of digital maps through GIS has provided an optimal means to store and manipulate soil variation data effectively (Khatri et al., 2019; Moukrim et al., 2022).

## Irrigation system design and distribution

In this study, drip irrigation is simulated in HYDRUS-2D software as shown in Figure 3. The simulation was performed within a square domain, located in a vertical plane at Saknia site, with dimensions of 460 cm in width and 400 cm in depth.

The drip irrigation system is represented by two drippers spaced of 260 cm and serving as water supply (see top of Figure 3). A water tank delivers water to the system with a flow rate of 1.065 L/h per dripper, which correspond to a water flux of $q$ = 0.56 cm/h. No-flux boundary conditions were applied to both the right and left sides of the soil profile, assuming symmetry in the soil water pressure head within and outside the geometry domain. A free drainage boundary condition was imposed at the bottom of the profile.

Initial input data required for HYDRUS-2D includes initial volumetric water content $\theta_i$= 0.012 cm³·cm⁻³ (Table 1) and hydrodynamic parameters ($\theta_r$, $\theta_s$, $n$, $a$, $K_s$, $\eta$) (Table 2).

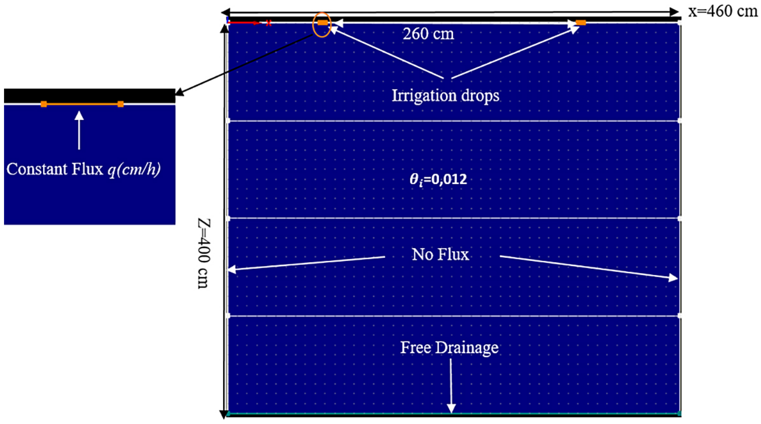


**Figure 3.** Domain geometry used in the HYDRUS-2D

## RESULTS AND DISCUSSION

Understanding soil types at various depths is essential. This information is crucial in agronomy, where soil texture affects plant growth and water retention, as well as in civil engineering. Figure 4 presents the grain-size distribution and texture of the soil in the Maâmora forest and cumulative mass, covering a depth range of 0–80 cm. Clay (< 2 µm): There is no clay content in the soil (0% mass percentage). Loam (2–50 µm): The mass percentage for loam particles is minimal, with the highest being 2.33% at 30 µm. Sand (50–2000 µm): Sand particles dominate the soil composition. The peak mass percentage is at 200 µm with 68.764%. Other significant sand fractions are at 250 µm (18.928%), 500 µm (3.053%), and 800 µm (0.62%). The cumulative mass percentage curve (black line) rises steeply and then reaches plateau, indicating that the majority of the soil mass is composed of sand-sized particles. By the time the particle size reaches approximately 250 µm, the cumulative mass percentage is already close to 100%, showing that most of the soil mass is accounted for by particles smaller than this size. Thus, it can be concluded that the studied soil is homogeneous within the depth range of 0–80 cm (Figure 5).

Figure 6 represents the spatial interpolation of sand percentages in Maâmora forest soils at different depths: 0–20 cm, 20–40 cm, 40–60 cm and 60–80 cm. At a of depth 0–20 cm, sand percentages vary slightly across the region, with areas in the west showing lower sand content (around 95–96%) and central and eastern areas showing higher values (97–98%). This reflects a predominantly sandy texture at the surface, but with variations due to local inputs or environmental

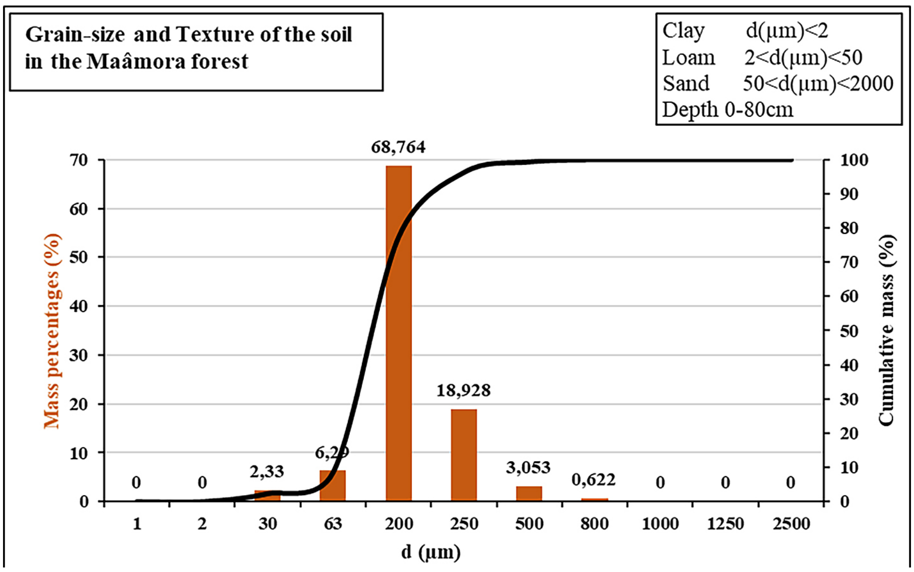


**Figure 4.** Grain-size, texture and cumulative mass (%) of the soil in the Maâmora forest

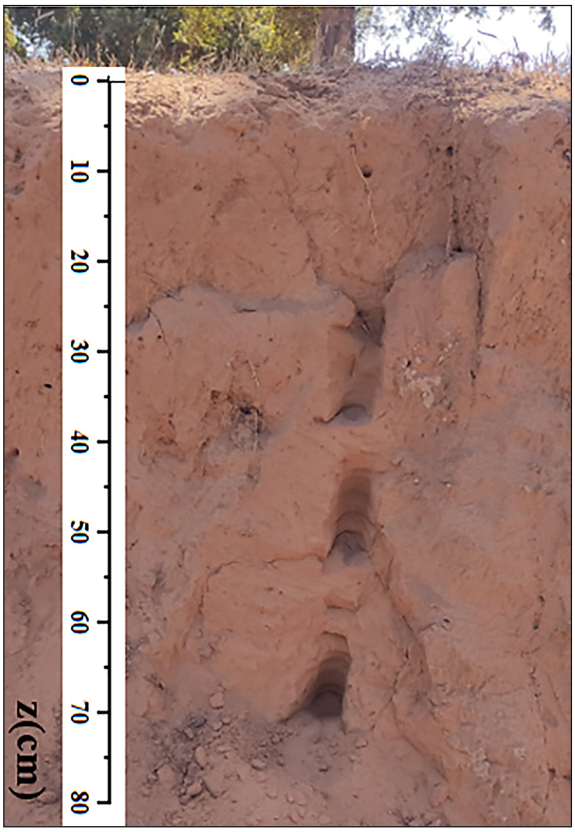


**Figure 5.** The sandy soil depth (0–80 cm) in the Maâmora forest

conditions. At a of depth 20–40 cm, at this depth, sand content increases overall compared to the surface. Areas to the southeast, especially around Sidi Allal El Bahraoui, show maximum values (98–99%), suggesting very sandy soils. Areas to the northwest maintain a slightly lower proportion, but remain largely dominated by sand. At a depth of 40–60 cm, soils become even sandier at depth, with percentages approaching or exceeding 98% in most areas. Central and eastern areas show a marked uniformity in the sandy texture, indicating an increased dominance of coarse particles at this depth. At a depth of 60–80 cm, the distribution remains strongly sandy, with sand percentages close to 98–99% throughout most of the region. Areas to the southwest and southeast (Arjate and Sidi Allal El Bahraoui) show slightly higher values, highlighting the predominance of sand throughout the depth of the profile.

Figure 7 presents a series of thematic maps illustrating the spatial distribution of the Loam fraction (%) at various soil depths (0–20 cm, 20–40 cm, 40–60 cm, and 60–80 cm) in the Maâmora region of Morocco. At a depth of 0–20 cm, silt is concentrated primarily in the central and southern areas, with values ranging from 1% to 5%,

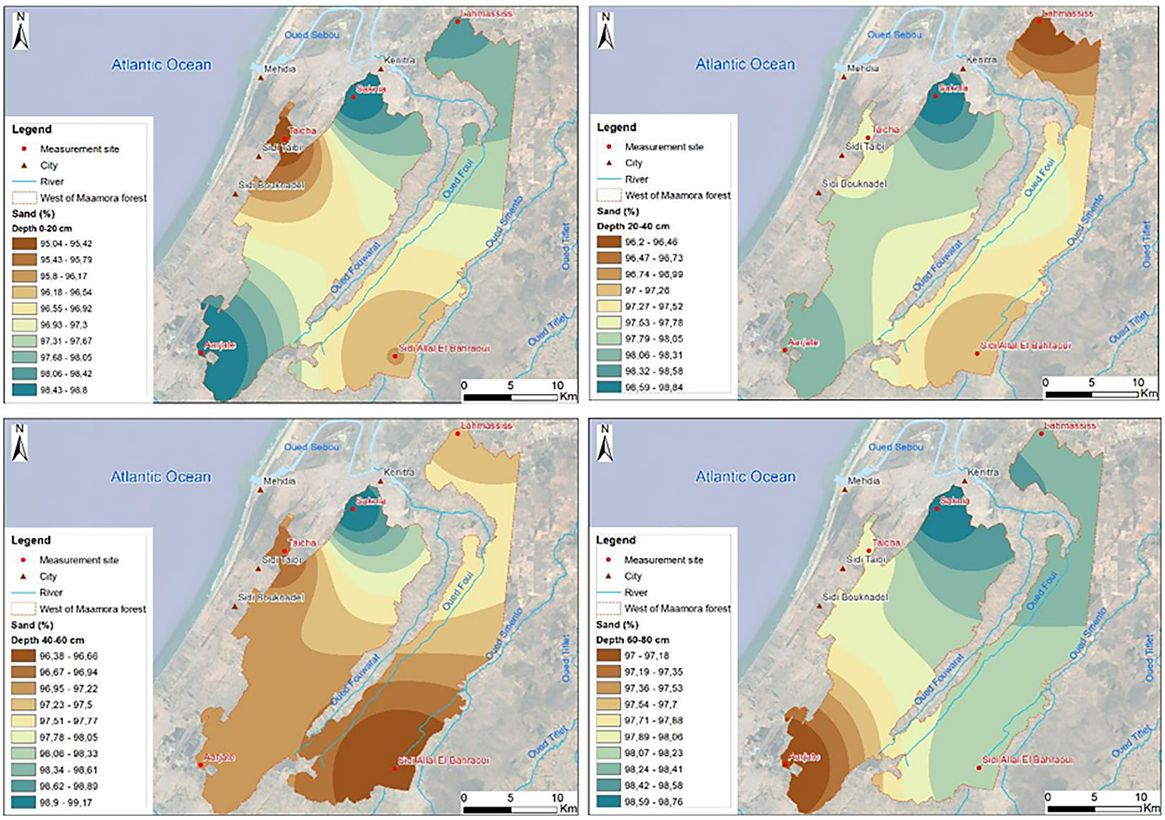


**Figure 6.** Spatial interpolation of sand percentages in Maâmora forest soils at different depths: 0–20 cm, 20–40 cm, 40–60 cm and 60–80 cm

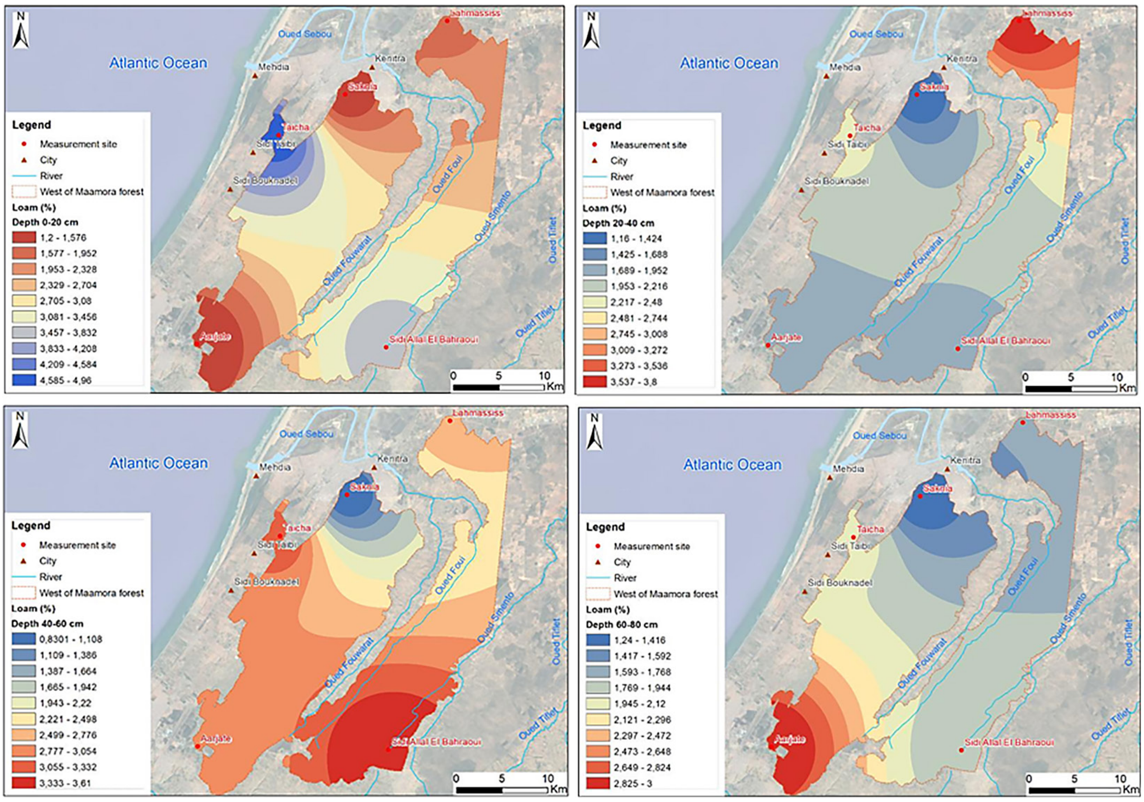


**Figure 7.** Spatial interpolation of loam percentages in Maâmora forest soils at different depths: 0–20 cm, 20–40 cm, 40–60 cm and 60–80 cm

indicating a minimal contribution of silt to the soil texture. At a depth of 20–40 cm, a decrease in silt is observed in some areas, likely due to leaching, while the coastal and southeastern regions remain poor in silt (< 2%). At depths of 40–60 cm and 60–80 cm, the percentage of silt decreases progressively with depth, reaching very low levels (< 1%) in most areas. On the basis of the analysis of Figures 6 and 7, it is evident that the soil in the Maâmora forest is predominantly sandy.

The data presented in Table 2 and the calculated constant water flux $q$(cm/h) were used for simulating water movement in soils. In this case, the HYDRUS-2D software with the Van Genuchten model were used to represent water content, predict water flow profiles, and understand water movement in the soil by drip irrigation. Figure 8 shows the simulation of water content (θ) as a function of depth $z$(cm) and horizontal distance $x$(cm) at different times (50 h, 100 h, 200 h, 400 h) under drip irrigation. The variation of the infiltration flux shows a typical behavior of water infiltration in a soil, with both vertical (downward) and horizontal (lateral) propagation. As time passes, the water infiltrates deeper and covers a larger surface area. After 50 hours, it was observed that the moisture reaches a depth of approximately 55 cm, with a slight increase in moisture horizontally, at 100 hours, the moisture depth reaches approximately 100 cm. The increase in the wetland indicates that the water begins to be distributed in a more uniform manner, reaching new layers of the ground. At 200 hours, humidity contours show more significant growth both in depth and in width, indicating a deeper infiltration of water in the soil. After 400 hours, the wet areas under each dripper are nearly flush. Moisture has penetrated deep and laterally, reaching a depth of approximately 240 cm. Taking into account the fact that the wet areas under each dripper are starting to move closer together, the spatial evolution of moisture under the influence of two drippers is observe in a scenario where moisture propagates significantly in depth and laterally in the long term. This explains that the soil under study is sandy, as illustrated in Figure 8. Through this study, it can be said that plant roots or the soil between the drippers are beginning to benefit from increased moisture.

Figure 9 illustrates the results of water content variation as a function of depth (cm) (Fig. 9a) and horizontal distance $x$ (cm) (Fig. 9b) at

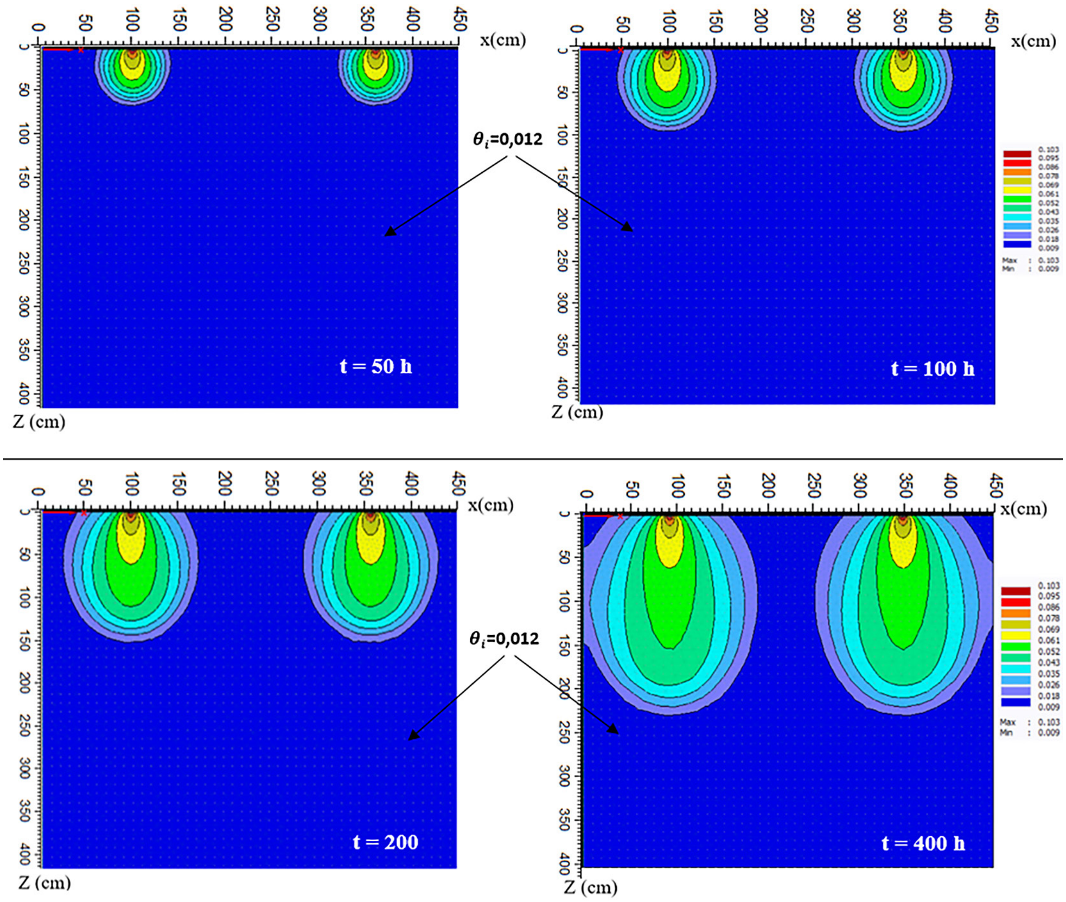


**Figure 8.** Simulation of water content (θ) as a function of depth $z$(cm) and horizontal distance $x$(cm) at different times (50 h, 100 h, 200 h, 400 h) under drip irrigation

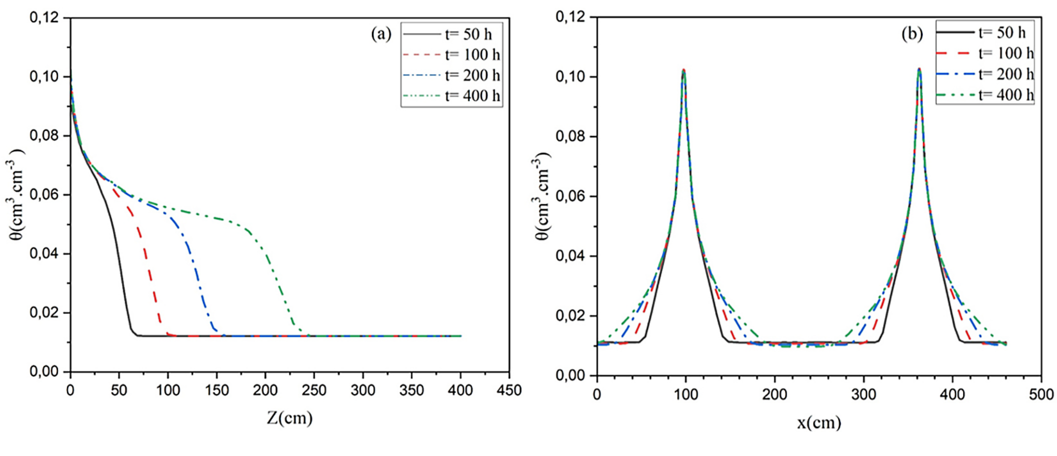


**Figure 9.** (a), Water content as a function of depth (cm) and (b), horizontal distance (cm) at different times (t = 50 h, t = 100 h, t = 200 h, and t = 400 h) under drip irrigation in the study area

different time intervals (t = 50 h, t = 100 h, t = 200 h, and t = 400 h, revealing significant insights into the water distribution under drip irrigation in the study area.

The spatial evolution of moisture under the influence of two drippers is clearly observed, the water content exhibits a decreasing trend with increasing soil depth across all time intervals (Figure 9a). This behavior reflects the vertical infiltration of water from the emitter, where the highest water content is observed near the surface. At $t$ = 50 h, the wetting front is shallow, indicating that water infiltration is concentrated in the upper soil layers. As time progresses, at t = 100 h and t = 200 h, the wetting front deepens, with water content gradually increasing in deeper soil layers. By t = 400 h, the wetting front reaches its maximum depth, and water content in the upper layers stabilizes, suggesting that equilibrium has been achieved near the emitter zone. This temporal evolution highlights the impact of soil hydraulic properties on water movement, with the infiltration rate determining the extent of water penetration over time. The observed pattern also indicates the effectiveness of drip irrigation in maintaining soil moisture near the root zone while minimizing deep percolation losses. Water content decreases with increasing horizontal distance from the emitter at all-time intervals (Figure 9b). At t =50 h, the wetted zone is narrow, demonstrating limited lateral water spread during the early stages of irrigation. Over time, at t = 100 h and t = 200 h, the wetted area expands as water disperses outward. By t = 400 h, the wetted zone reaches its maximum extent, though the water content diminishes with increasing distance from the emitter; the wet areas under each dripper are starting to move closer together, the lateral spread of water is influenced by the soil texture and structure. Sandy soils typically exhibit faster infiltration rates with limited lateral movement, while finer-textured soils allow for greater horizontal dispersion. This lateral distribution ensures that the water is confined within the effective root zone, reducing water loss to the areas beyond the crop root system. It can be concluded that plant roots and the soil between the drippers benefit from the increased moisture in the sandy soil. This regular moisture uptake supports the roots of the Cork Oaks while ensuring that the necessary amount of water is utilized efficiently, preventing waste.

## CONCLUSIONS

The Maâmora forest, the world's largest cork oak (Quercus suber) forest, faces increasing tree mortality due to drought, urbanization, tree debarking, and overgrazing. Previous reforestation attempts have failed, primarily because young cork oaks could not withstand water stress and climate change effects. This study demonstrated that sustainable irrigation methods, particularly drip irrigation, are essential for improving seedling survival and overall forest resilience. Using GIS-based soil mapping and HYDRUS-2D numerical modeling, the study analyzed soil properties in five sites, revealing a predominantly sandy texture with low initial moisture content. Drip irrigation simulations showed efficient water distribution, with moisture reaching depths of up to 240 cm after 400 hours, ensuring adequate hydration for young cork oaks. These results highlight the necessity of integrating soil characterization, spatial analysis, and numerical modeling to develop targeted irrigation strategies. In conclusion, this research underscored the role of GIS and HYDRUS-2D in optimizing water use efficiency and reducing seedling mortality in reforestation efforts. By adopting data-driven irrigation techniques, the sustainability and resilience of the Maâmora forest can be enhanced in the face of ongoing climate challenges.

## REFERENCES

1. Aronson, J., Pereira, J.S., Pausas, J.G. (2009). In cork oak woodlands on the edge society for ecological restoration international. *Island Press, 36*(8).
2. Benabou, A., Moukrim, S., Laaribya, S., Aafi, A., Chkhichekh, A., El Maadidi, T., & El Aboudi, A. (2022). Mapping ecosystem services of forest stands: case study of Maâmora, Morocco. *Geography, Environment, Sustainability, 15*(1), 141–149. https://doi.org/10.24057/2071-9388-2021-047
3. Ballais, J. L., Chave, S., Delorme-Laurent, V., & Esposito, C. (2007). Hydro géomorphologie et inondabilité. *Géographie physique et Quaternaire, 61*(1), 75–84.
4. Boukbida, H., Nabil, A., El Ghaddari, H.M., Smaili, L., & Grimaldi, M. (2016). *Caractérisation du sol de la subéraie et des plantations d'eucalyptus de la Maâmora au Maroc*. 1–38.
5. Brooks, R.H., & Corey, C.T. (1964). *Hydraulic properties of porous media*. Hydrology Paper, Colorado State University, Fort Collins, 3.
6. Brunetti, G., Papagrigoriou, I.A., & Stumpp, C. (2020). Disentangling model complexity in green roof hydrological analysis: A Bayesian perspective. *Water Research, 182*(9), 115973. https://doi.org/10.1016/j.watres.2020.115973
7. Bufon, V. B., Lascano, R. J., Bednarz, C., Booke, J. D., & Gitz, D. C. (2012). Soil water content on drip-irrigated cotton: Comparison of measured and simulated values obtained with the HYDRUS 2-D model. *Irrigation Science, 30*(4), 259-273. http://dx.doi.org/10.1007/s00271-011-0279-z
8. Bourziza, R., Hammani, A., Mailhol, J. C., Bouaziz, A., & Kuper, M. (2017). Modélisation de l'irrigation

en goutte à goutte enterré du palmier dattier sous les conditions oasiennes. *Cahiers Agricultures, 26*(3), 35007. https://doi.org/10.1051/cagri/2017023

9. Camilo-Alves, C., Dinis, C., Vaz, M., Barroso, J. M., & Ribeiro, N. A. (2020). Irrigation of young cork oaks under field conditions -Testing the best water volume. *Forests, 11*(1), 88. https://doi.org/10.3390/f11010088
10. Cherki, K. (2011). Analyse de la répartition spatiale des incendies de forêt en fonction des facteurs anthropiques, écologiques et biophysiques: Le cas de la forêt de la Maâmora (Maroc septentrional). *Open Edition Journals, 20*(20), 1–33. https://doi.org/10.4000/etudescaribeennes.10978
11. Fatehnia, M., Tawfiq, K., & Abichou, T. (2014). Comparison of the methods of hydraulic conductivity estimation from mini disk infiltrometer. *Electronic Journal of Geotechnical Engineering, 19*, 1047–1063.
12. Ghouldan, A., Benhoussa, A., & Ichen, A. (2024). Evolution of land use/land cover in Mediterranean forest areas: A case study of the Maâmora in the North-West Morocco. *Ecological Engineering & Environmental Technology, 25*(10), 134–149. https://doi.org/10.12912/27197050/191413
13. Gliti, O., Igouzal, M., & El Idrissi, M. C. (2023). Development of a sustainable solar water desalinator using a novel hollow hemispherical grid shell solar selective absorber designed via phasor particle swarm algorithm. *Ecological Engineering & Environmental Technology, 24*(9), 130–149. https://doi.org/10.12912/27197050/173510
14. Giuseppe, P. (2007). Using HYDRUS-2D simulation model to evaluate wetted soil volume in subsurface drip irrigation systems. *Journal of Irrigation and Drainage Engineering, 133*(4), 342–349. http://dx.doi.org/10.1061/(ASCE)0733-9437(2007)133:4(342)
15. Hracherrass, A., Berkat, O., De Montard, F. X. (2009). Implications des choix alimentaires des ovins et des bovins dans les parcours à Teline linifolia pour l'aménagement de la subéraie de la Mâamora (Maroc). *Cahiers Agricultures, 18*(1), 35–43.
16. Khatri, S., & Suman, S. (2019). Mapping of soil geotechnical properties using GIS. *Indian Conference on Geotechnical and Geo-Environmental Engineering*, 1–4.
17. Laaribya, S. (2006). Il faut sauver la forêt de la Maâmora (Maroc). *Forêt Méditerranéenne,* XXVII (1), 65–72.
18. Laaribya, S., Alaoui, A., Ouhaddou, H., Ayan, S., & Bijou, M. (2021). Prediction by maximum entropy of potential habitat of the cork oak (Quercus suber L.) in Maâmora Forest, Morocco. *Forestist, 71*(2), 63–69. http://dx.doi.org/10.5152/forestist.2021.20059
19. Lemkimel, Z., & Daiboun, T. (2024). Impact of urban dynamics and climate change on forest areas: The Maâmora forest in the city of Kenitra, Morocco. *Multidisciplinary Science Journal, 6*(7), 2024123.
20. Mitique, A., Hachimi, M., Qanza, H., Hmimou, A., & Igouzal, M. (2024). Hydraulic modeling in the vadose zone of an agricultural area under water stress (M'nasra, Morocco). *Russian Meteorology and Hydrology, 49*(10), 888–895. http://dx.doi.org/10.3103/S1068373924100066
21. Moukrim, S., Benabou, A., Lahssini, S., Aafi, A., Chkhichekh, A., Moudden, F., Ben Bammou, M., & El Aboudi, A. (2022). Spatio-temporal analysis of North African forest cover dynamics using time series of vegetation indices: Case of the Maâmora forest (Morocco). *Biosystems Diversity, 30*(4), 372–379. http://dx.doi.org/10.15421/012236
22. Poeiras, A. P., Silva, M. E., Günther, B., Vogel, C., Surový, P., & Ribeiro, N. (2021). Cork influenced by a specific water Regime-Macro and microstructure characterization: The first approach. *Wood Science and Technology, 55*(4), 1653–1672. https://doi.org/10.1007/s00226-021-01334-1
23. Qanza, H., Maslouhi, A., Hachimi, M., & Hmimou, A. (2018). Inverse estimation of the hydrodispersive properties of unsaturated soil using complex-variable-differentiation method under field experiments conditions. *Eurasian Soil Science, 51*(10), 1229–1239. https://doi.org/10.1134/S1064229318100101
24. Šimůnek, J., Brunetti, G., Jacques, D., van Genuchten, Th., & Šejna, M. (2024). Developments and applications of the HYDRUS computer software packages since 2016. *Vadose Zone Journal, 23*(4), 1-25. http://dx.doi.org/10.1002/vzj2.20310
25. Šimůnek, J., & van Genuchten, M.T., & Šejna, M. (2006). *The Hydrus Software Package for simulating two- and three-dimensional movement of water, heat, and multiple solutes in variably-saturated media*. PC Progress: Prague, Czech Republic, Version 1, 241.
26. Skaggs, A. T., Trout, T., Šimůnek, J., & Shouse, P. (2004). Comparison of HYDRUS-2D simulations of drip irrigation with experimental observations. *Journal of Irrigation and Drainage Engineering, 130*(4), 304–310. http://dx.doi.org/10.1061/(ASCE)0733-9437(2004)130:4(304)
27. Serrasolses, I., Pérez-Devesa, M., Vilagrosa, A., Pausas, J.G., Sauras, T., Cortina, J., Vallejo, V. R. (2009). Soil properties constraining cork oak distribution. *Scientific Bases for Restoration and Management, 8*, 89–101.
28. Van Genuchten, M. T., Naveira-Cotta, C., Skaggs, T. H., Raoof, A., & Pontedeiro, E. M. (2014). The use of numerical flow and transport models in environmental analyses. *Application of soil physics in environmental analyses*, 349–376. https://doi.org/10.1007/978-3-319-06013-2_15
29. Vdović, N., Obhođaš, J., Pikelj, K. (2010). Revisiting the particle-size distribution of soils: comparison of different methods and sample pre-treatments. *European Journal of Soil Science, 61*(6), 854–864.